Table 7 Relationship between degree of PEGylated-Hexon and adenovirus vector size

Ratio (Ad:PEG)*	PEG modification ratio (%)	Vector size (nm)	Serum half-life (min)
1:0	0	113.3±0.76	1.6
1:25	10	120.6±0.64	1.8
1:100	34	123.8±0.98	1.8
1:400	61	128.5±1.25	5.0
1:1600	89	137.6±0.91	12.0
1:6400	100	148.2±1.48	78.6

*; Amount of PEG to lysine residue of adenovirus vector capsid protein (mol : mol)

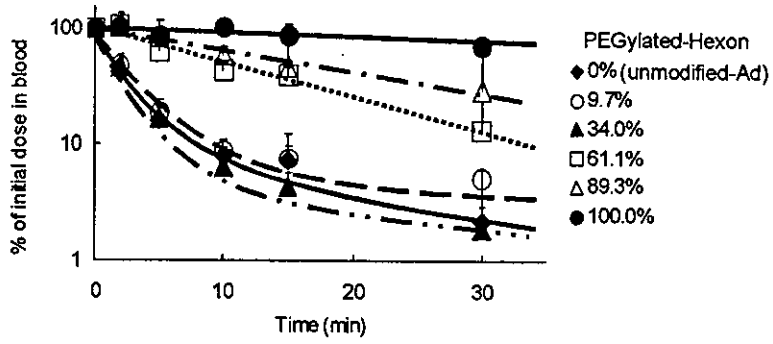

Fig. 42 Pharmacokinetics of PEGylated adenovirus vectors.
Normal female BALB/c mice were administrated intravenously with $1x10^{10}$ particles of unmodified-Ad or PEG-Ads. Blood samples were drawn at different times. The concentration of adenovirus vectors in serum was quantitated with southern blot method. A standard curve was made for each PEG-Ads. Each point was represented as mean ±S.D. (n=4).

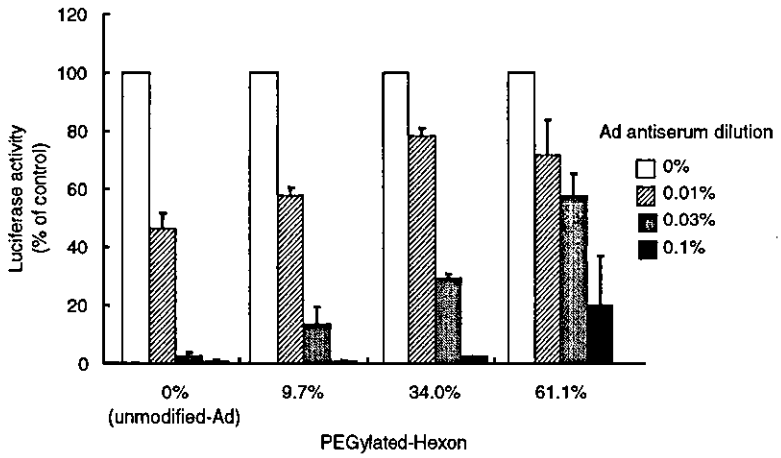

Fig. 43 Transduction of A549 cells by PEGylated adenovirus vectors in the presence or absence of adenovirus vectors antiserum.
A549 cells ($1x10^4$ cells) were tranceduced with 1000 particles/cell of unmodified-Ad or PEG-Ads in the presence or absence of Ad antiserum respectively. Luciferase expression was measured after 24 hr. Each point was represented as mean ±S.D. (n=3).

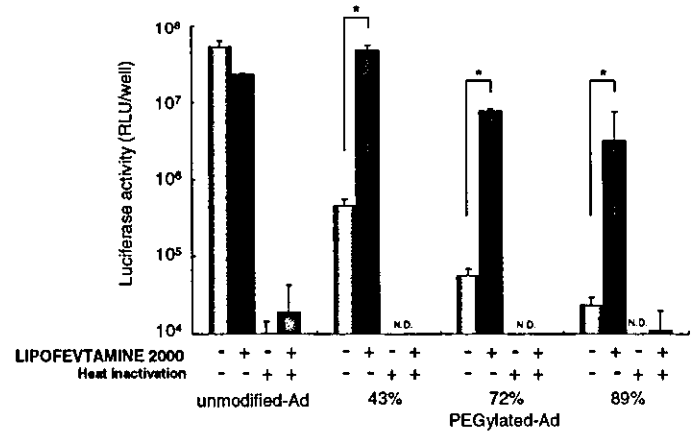

Fig. 44 Transduction efficiency of PEGylated adenovirus vectors into A549 cells in the presence or absence of LIPOFECTAMINE 2000.
A549 cells ($2x10^4$ cells) were transduced with 1000 particles/cell of unmodified or PEGylated Ad-Luc in the presence or absence of 20 μ g/ml of LIPOFECTAMINE 2000. After 4 hr, the virus solution was replaced with fresh medium, and the cells were incubated for 24 hr. Luciferase expression was measured. Each point represents the mean ± S.D. (n=3). * $P<0.05$ (*t-test*).

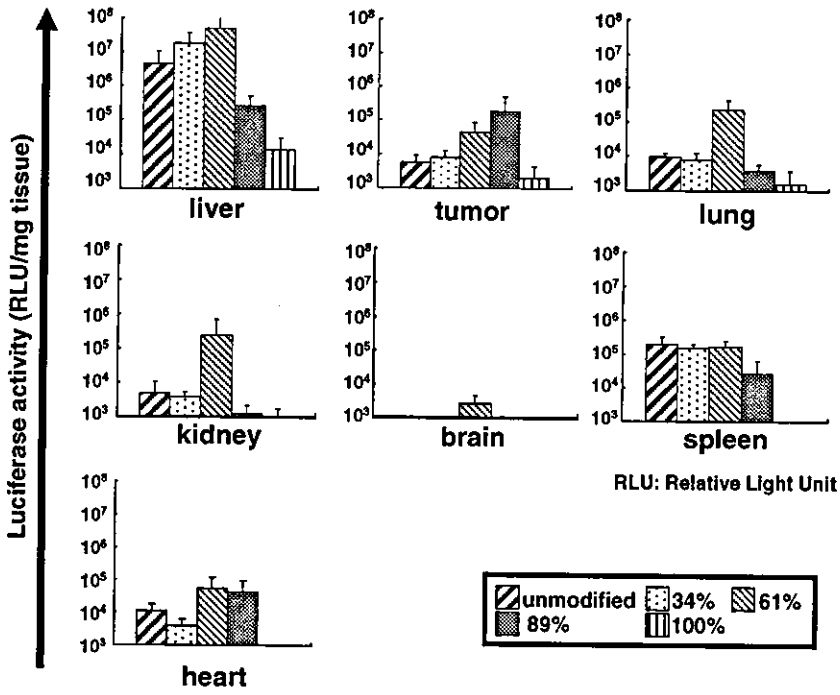

Fig. 45 ***In vivo*** **gene expression pattern of PEG-Ad after i.v. administration into mice.** 2×10^6 Meth-A fibrosarcoma tumor cells were inoculated intradermally and 10^{10} particles of unmodified or PEGylated Ad-Luc were injected intravenously after approximately one week. After 2 days, organs were harvested and homogenized with buffer. Luciferase activity was then measured using the kit according to the manufacture's instructions.(n=4).

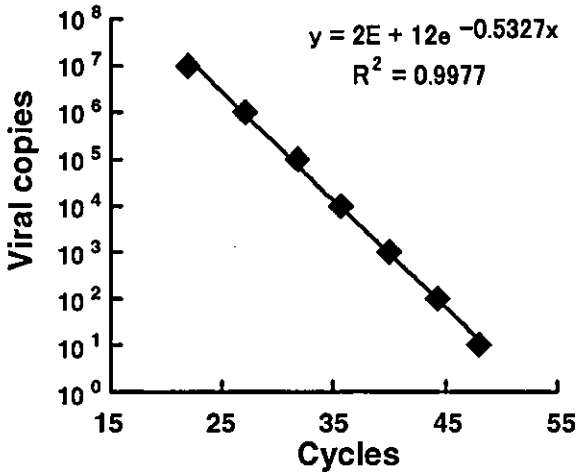

Fig. 46 Standard curve of TaqMan Real-time PCR

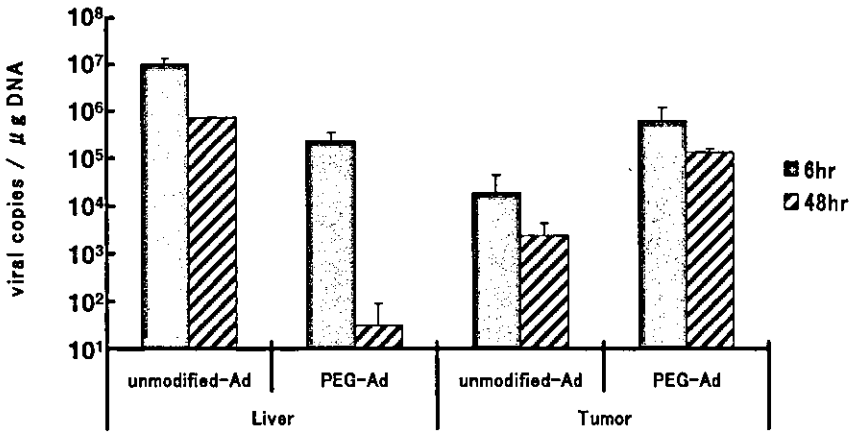

Fig. 47 Accumulation of Ad particles in tumor, and reduction in liver induced by PEGylation.
Real-time PCR was carried out for detecting viral particles existence in tumor and liver 6, 48 h after systemically administration of 1 x 10^{11} VP of both unmodified-Ad and PEGylated Ad (89% of modification ratio).

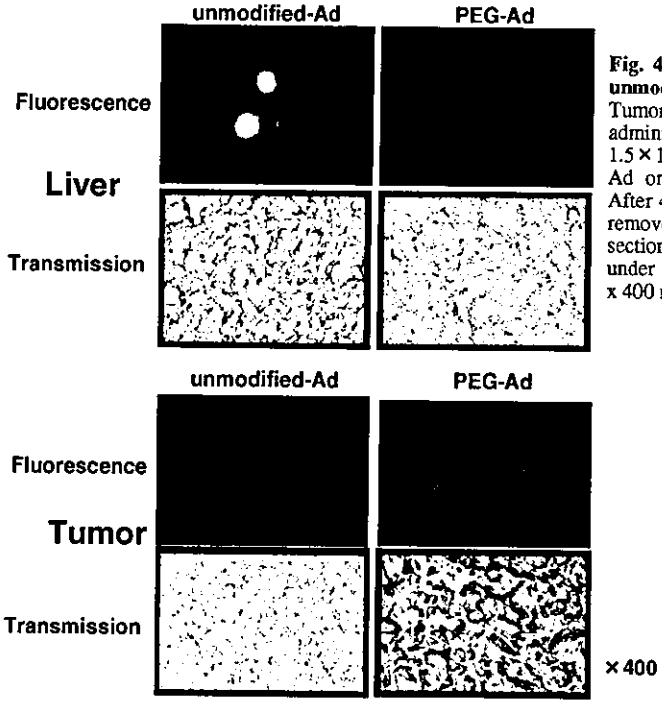

Fig. 48 EGFP gene expression of unmodified-Ad and PEG-Ad.
Tumor-bearing mice were administrated intravenously with 1.5×10^{11} particles of unmodified-Ad or PEG-Ad expressing EGFP. After 48 hr, livers and tumors were removed, processed for frozen sectioning. EGFP was observed under a fluorescence microscopy at x 400 magnification.

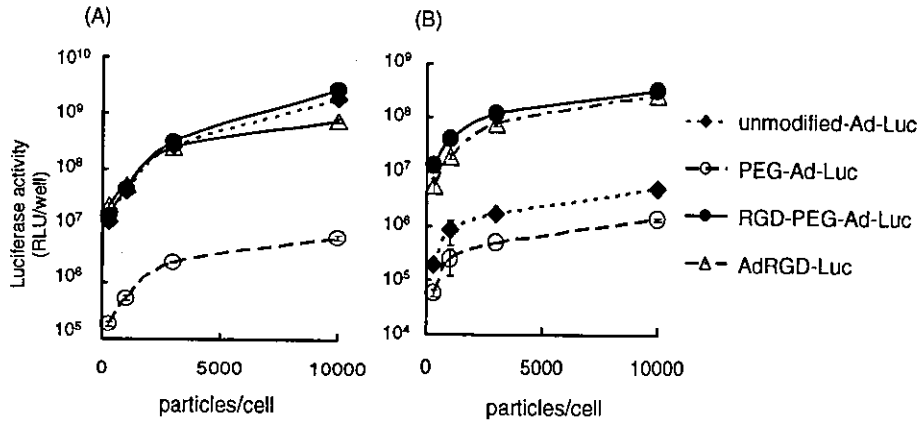

Fig. 49 Transduction of A549 cells and B16BL6 cells by RGD-PEGylated adenovirus vectors
(A) A549 cells and (B) B16BL6 cells ($2x10^4$ cells) were transfected with 300, 1000, 3000 or 10000 particles/cell of Ad, PEG-Ad-Luc, RGD-PEG-Ad-Luc or AdRGD-Luc respectively. Luciferase expression was measured after 24 hr. Each point was represented as mean ±S.D.

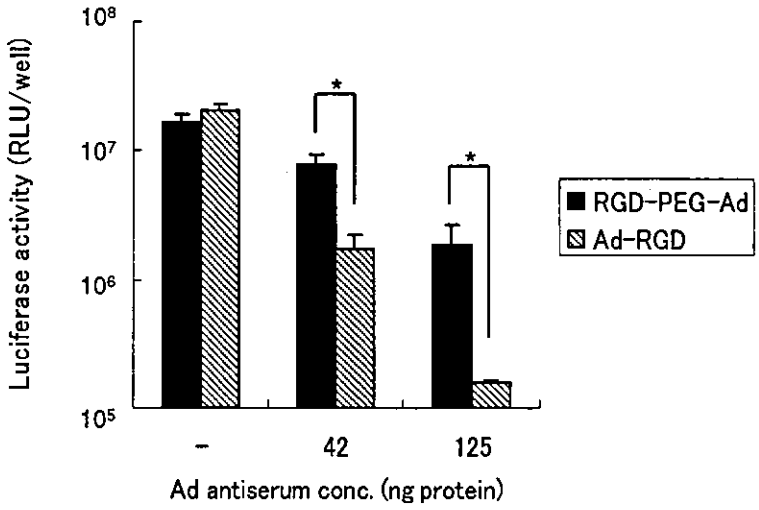

Fig. 50 Transduction of B16BL6 cells by RGD-PEGylated adenovirus vectors in the presence or absence of adenovirus vectors antiserum.
B16BL6 cells ($2x10^4$ cells) were tranceduced with 1000 particles/cell of RGD-PEG-Ad or AdRGD in the presence or absence of Ad antiserum respectively. Luciferase expression was measured after 24 hr. Each point was represented as mean ±S.D. (n=3).

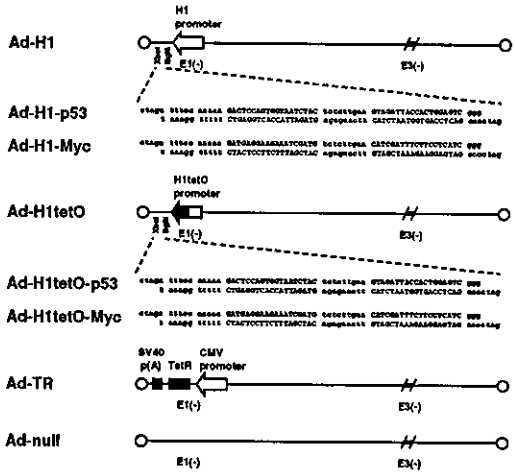

FIG. 51 The structure of Ad vectors used in the present study.
The H1 promoter-based siRNA expression cassette was inserted into the E1 deletion region of Ad genome. For the inducible siRNA expression, a tetracycline operator (tetO) sequence was introduced in the downstream of the TATA box in the H1 promoter, as described in MATERIALS AND METHODS section. The target sequences against the p53 and c-myc gene were shown in a large letter. Ad-TR is the Ad vector containing a tetracycline repressor sequence under the control of the CMV promoter/enhancer. Ad-null is the Ad vector without foreign genes in the E1 deletion region.

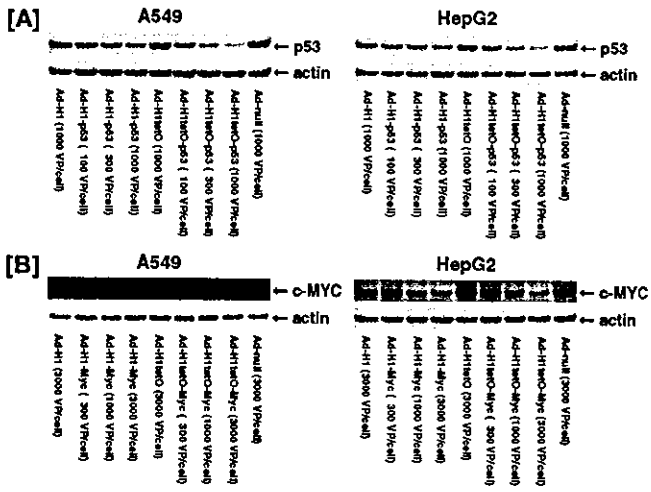

FIG. 52 The dose-dependent suppression of the p53 and c-MYC expression by Ad vector-delivered siRNA.
A549 and HepG2 cells were infected with each Ad vector for 1.5 hr, and then cultured for 3 days. The proteins were then extracted from the cells, and the levels of p53 (panel A) and c-MYC (panel B) expression were examined by Western blotting. The actin bands served as an internal control for equal total protein loading.

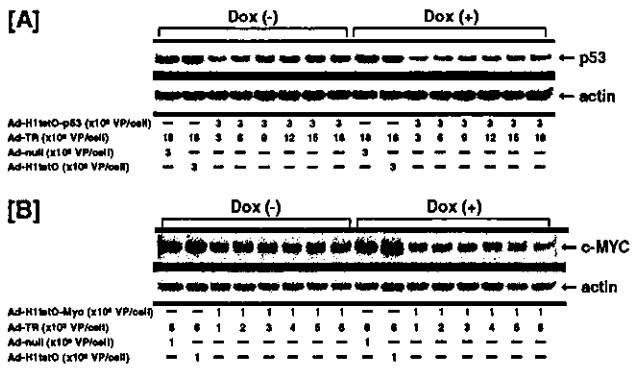

FIG. 53 Regulated suppression of the p53 and c-MYC expression by the co-infection of Ad-H1tetO-p53 or Ad-H1tetO-Myc plus Ad-TR. A549 cells were infected with the indicated amounts of Ad-H1tetO-p53 or Ad-H1tetO-Myc plus Ad-TR for 1.5 hr, and then cultured with or without Dox (10 μg/ml) for 3 days. The cells were also infected with Ad-null or Ad-H1tetO plus Ad-TR. The proteins were then extracted from the cells, and the levels of p53 (panel A) and c-MYC (panel B) expression were examined by Western blotting. The actin bands served as an internal control for equal total protein loading.

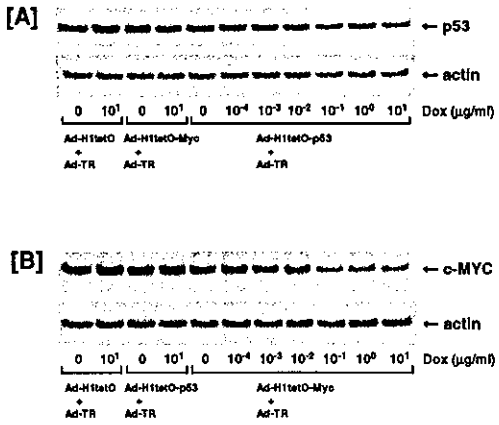

FIG. 54 Dox dose-dependent suppression of the p53 and c-MYC expression by the co-infection of Ad-H1tetO-p53 or Ad-H1tetO-Myc plus Ad-TR. A549 cells were infected with Ad-H1tetO-p53 (300 VP/cell) plus Ad-TR (1800 VP/cell) or Ad-H1tetO-Myc (1000 VP/cell) plus Ad-TR (6000 VP/cell) for 1.5 hr, and then cultured with various concentrations of Dox for 3 days. The cells were also infected with Ad-H1tetO plus Ad-TR. The proteins were then extracted from the cells, and the levels of p53 (panel A) and c-MYC (panel B) expression were examined by Western blotting. The actin bands served as an internal control for equal total protein loading.

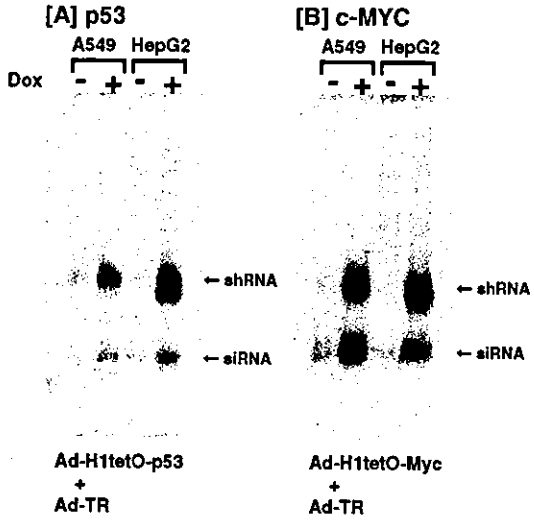

FIG.55 Dox inducible p53 or c-Myc siRNAs expression by the co-infection of Ad-H1tetO-p53 or Ad-H1tetO-Myc plus Ad-TR.
A549 and HepG2 cells were infected with Ad-H1tetO-p53 (300 VP/cell) plus Ad-TR (1800 VP/cell) or Ad-H1tetO-Myc (1000 VP/cell) plus Ad-TR (6000 VP/cell) for 1.5 hr, and then cultured with or without Dox (1 mg/ml) for 3 days. The total RNAs were then extracted from the cells, and the levels of p53 and c-myc siRNAs expression were examined by Northern blotting.

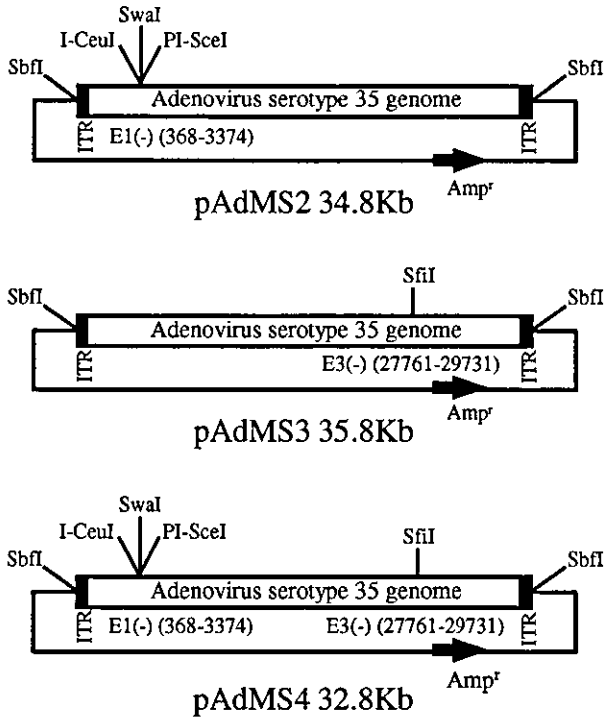

Fig. 56 The structure of the vector plasmids pAdMS2, -3, and -4 for construction of Ad35 vectors by the improved in vitro ligation method.

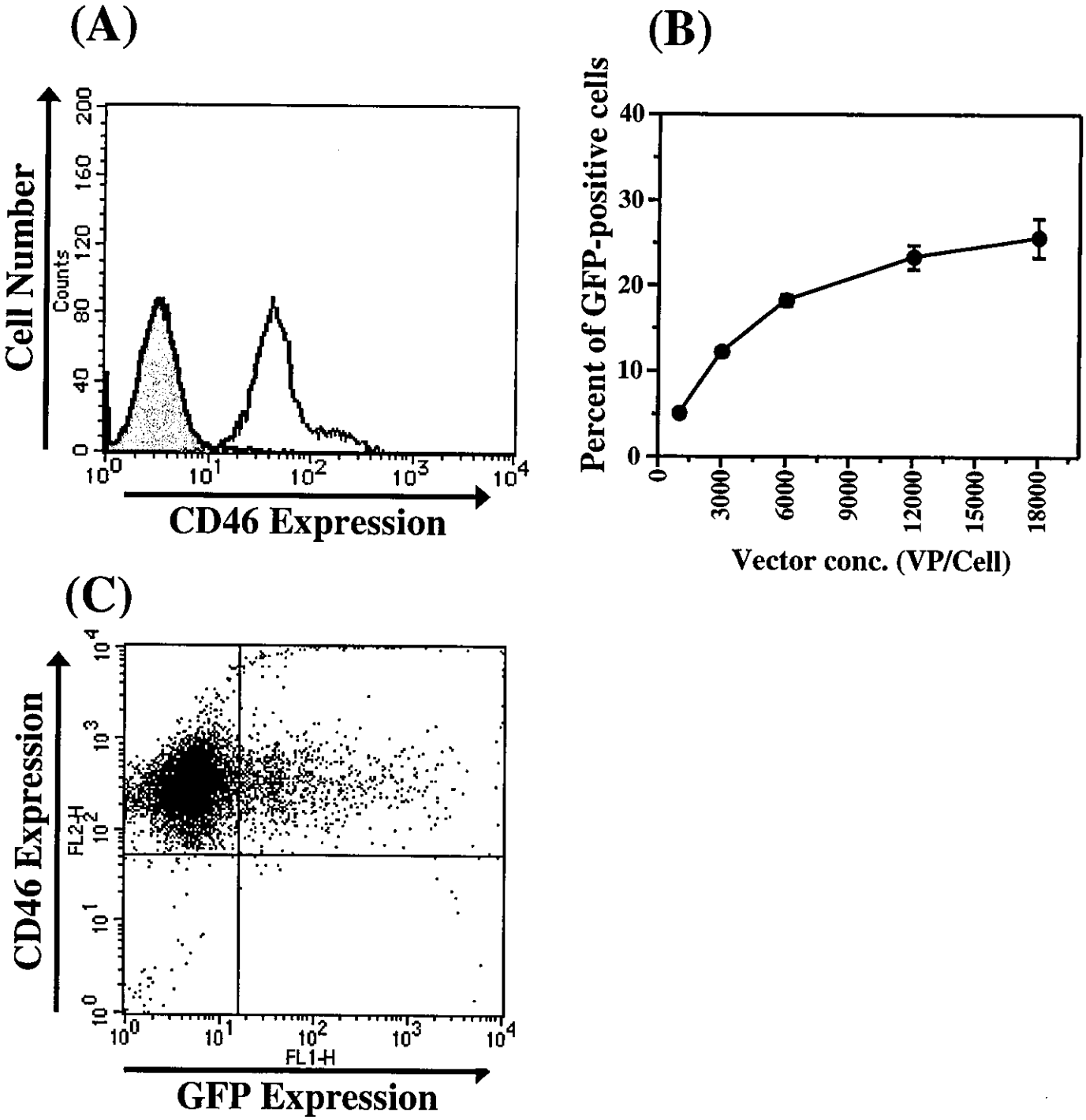

Fig. 57 (A) CD46 expression in human bone marrow CD34$^+$ cells. The cells were incubated with FITC-conjugated anti-CD46 antibody. As a negative control, the cells were incubated with an irrelevant antibody (shaded histogram). Similar levels of CD46 were found in the cells from three different donors. (B) Dose response of the percentage of GFP-positive cells following transduction with Ad35 vector containing a CMV promoter-driven GFP expression cassette. Human bone marrow CD34$^+$ cells were transduced with the Ad35 vector at the indicated vector concentrations for 6 hrs, washed, and resuspended in medium. Forty-eight hours later, GFP expression was measured by flow cytometry. All data represent the means ± S.D. of three experiments. (C) The relationship between the CD46 expression level on human bone marrow CD34$^+$ cells and GFP expression levels following Ad35 vector transduction. The cells were transduced with the Ad35 vector containing the CMV promoter at 6000 VP/cell for 6 hrs, washed and resuspended in the medium. After 48 hr of incubation and washing, the transduced cells were incubated with an anti-CD46 antibody. The cells were then washed, resuspended, and incubated with PE-conjugated second antibody. Data shown are from one representative experiment of the three performed.

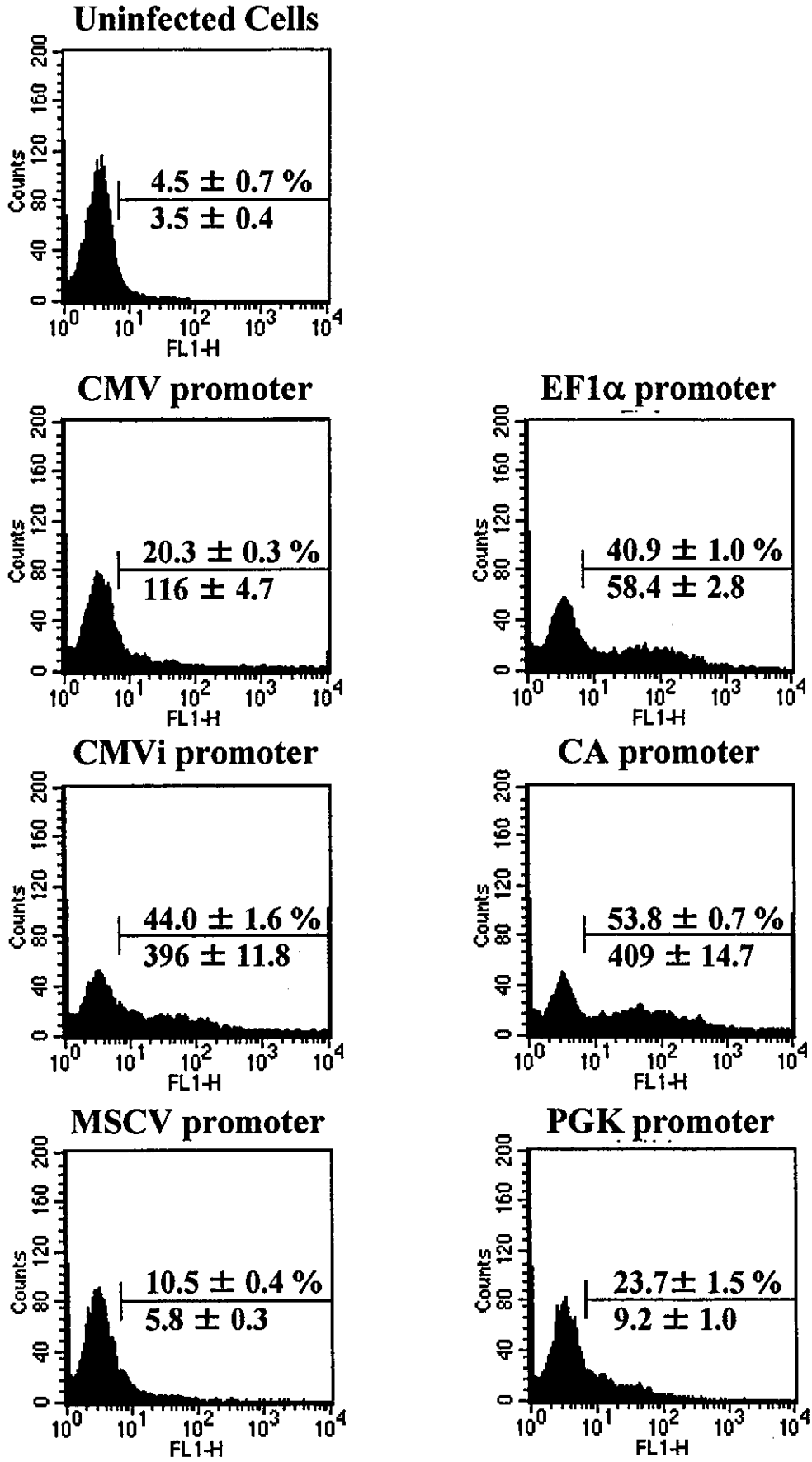

Fig. 58 Comparison of promoter activities in human bone marrow CD34$^+$ cells transduced with Ad35 vectors. The results are shown as a percentage of GFP-positive cells (upper) and the mean fluorescence intensity (MFI) (lower) in the panel. The CD34$^+$ cells were transduced with Ad35 vectors at 6000 VP/cell for 6 hrs, washed, and resuspended in medium. Forty-eight hours later, GFP expression was measured by flow cytometry. All data represent the means ± S.D. of three experiments.

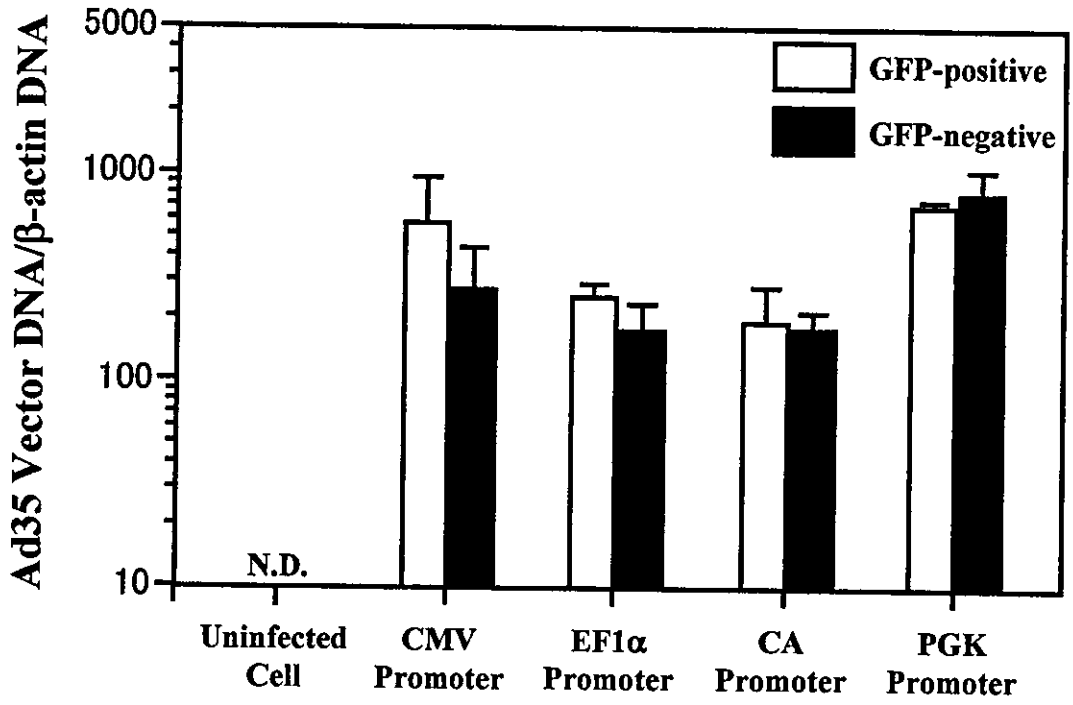

Fig. 59 Ad35 vector copy numbers in GFP-positive and GFP-negative cells following Ad35 vector transduction into human bone marrow CD34$^+$ cells. The CD34$^+$ cells were transduced with Ad35 vectors at 6000 VP/cell for 6 hrs, washed, and resuspended in medium. Forty-eight hours later, GFP-positive and GFP-negative cells were sorted and the total DNA was extracted from the cells. The copy numbers of Ad35 vectors and b-actin were analyzed by Taqman PCR. All data represent the means ± S.D. of two independent experiments. N.D., not detected (under the limit of detection).

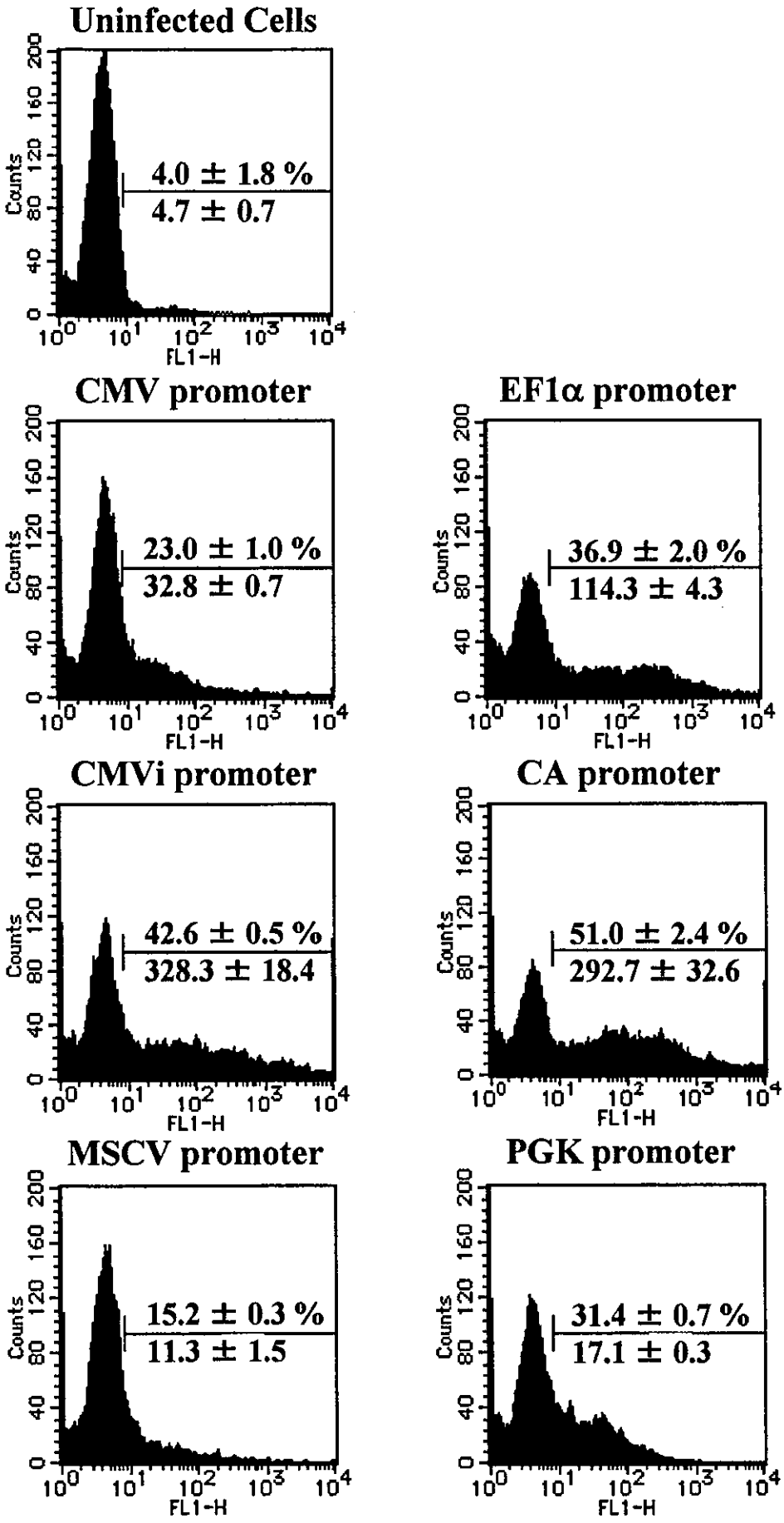

Fig. 60 Comparison of promoter activities in the $CD34^{+}CD38^{low/-}$ subsets transduced with Ad35 vectors. Results are shown as the percentage of GFP-positive cells (upper) and the mean fluorescence intensity (MFI) (lower) in the panel. The $CD34^{+}CD38^{low/-}$ subsets were transduced at 6000 VP/cell for 6 hrs, washed, and resuspended in medium. Forty-eight hours later, GFP expression was measured by flow cytometry. All data represent the means ± S.D. of two experiments.

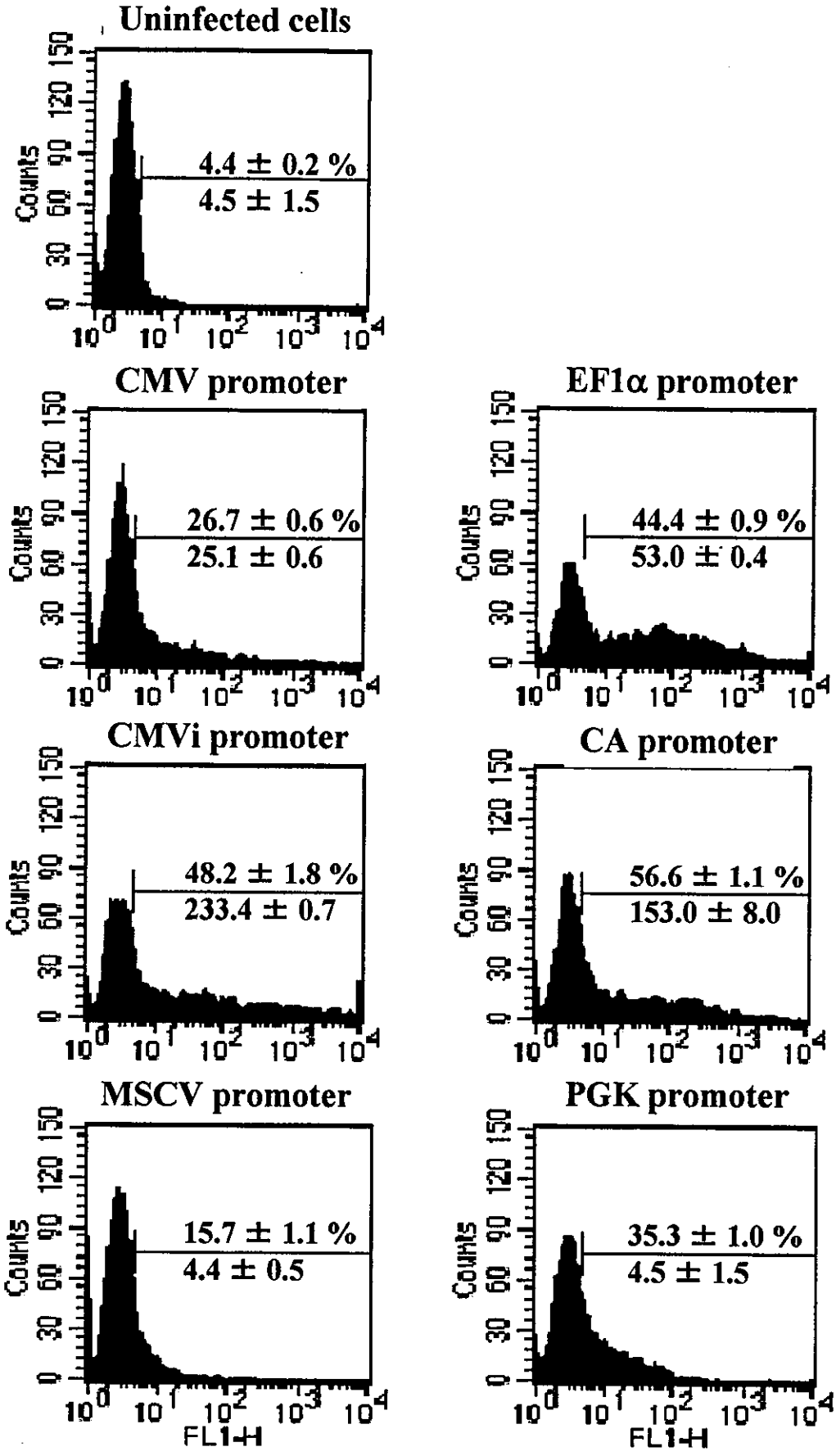

Fig. 61 Comparison of promoter activities in human bone marrow CD34$^+$AC133$^+$ subsets transduced with Ad35 vectors. Results are shown as the percentage of GFP-positive cells (upper) and the mean fluorescence intensity (MFI) (lower) in the panel. The CD34$^+$AC133$^+$ subsets were transduced at 6000 VP/cell for 6 hrs, washed, and resuspended in medium. Forty-eight hours later, GFP expression was measured by flow cytometry. All data represent the means ± S.D. of two experiments.

Table. 8 Numbers of colonies derived from GFP-positive and GFP-negative cells following transduction with the Ad35 vector containing the CA promoter in human CD34+ cells.

CD34+ cells		Total	BFU-E	CFU-GM	CFU-Mix
Sample 1	uninfected cells	222.8 ± 25.5	72 ± 11.8	150.3 ± 14.2	0.5 ± 0.6
	GFP-positive	193.5 ± 29 (86.9 %)	61 ± 9.9 (84.7 %)	131.5 ± 17.7 (87.5 %)	1 ± 1.4
	GFP-negative	180.5 ± 13.4 (81 %)	24.5 ± 0.7 (34 %)	155.5 ± 13.4 (103.5 %)	0.5 ± 0.7
Sample 2	uninfected cells	124.8 ± 13.5	44.5 ± 6.1	78.8 ± 9.5	1.5 ± 0.6
	GFP-positive	115 ± 11.3 (92 %)	29 ± 5.7 (65.2 %)	85.5 ± 6.4 (108.5 %)	0.5 ± 0.7
	GFP-negative	158 ± 19.8 (127 %)	26 ± 0 (58.4 %)	130.5 ± 20.5 (165.6 %)	1.5 ± 0.7

The data represent the mean number of colonies ± S.D. from duplicate cultures and the percentage of number of colonies/uninfected cells.

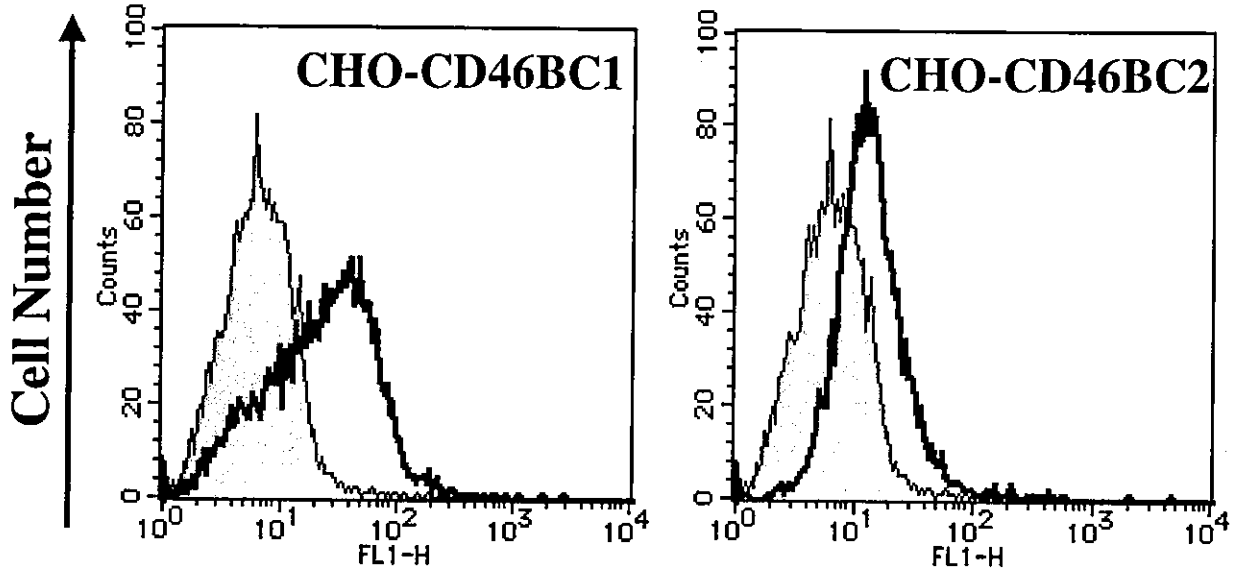

Fig.62 Human CD46 expression levels in CHO cell transfectants. The expression of CD46 on CHO cells transfected with cDNAs encoding the BC1 and BC2 idoforms of CD46 was investigated by using flow Cytometry with the monoclonal anti-CD46 antibody. CD46 expression level on wild type CHO cell were shown as shaded histogram.

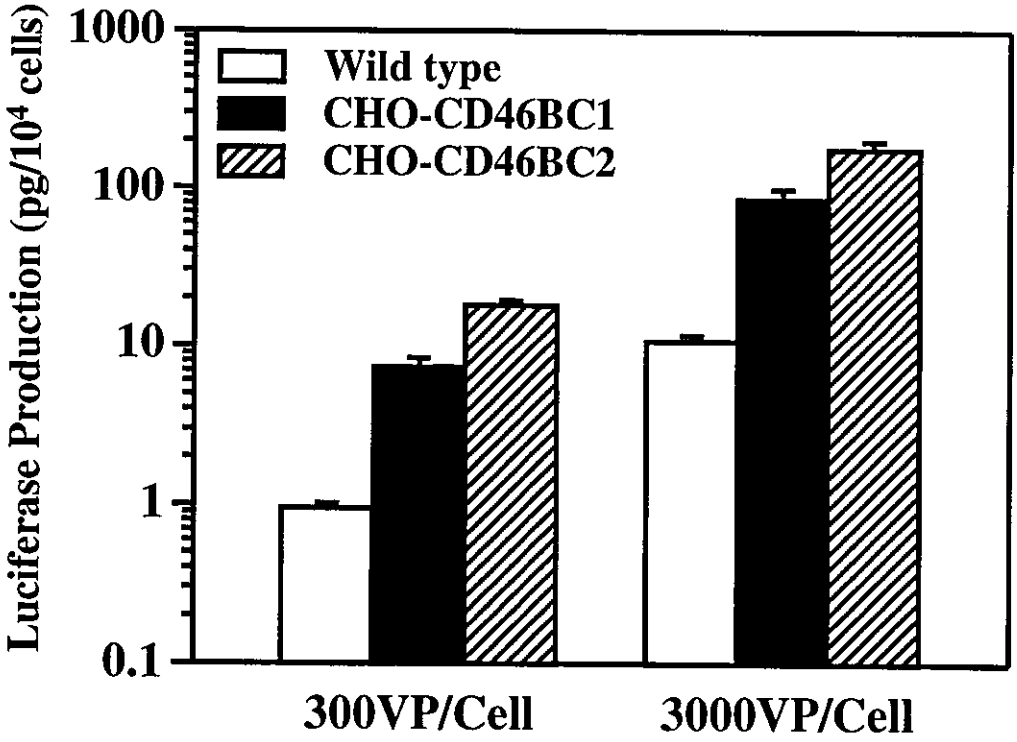

Fig.63 Ad35 vector-mediated Transduction into CHO Cells Expressing Human CD46. CHO cell and CHO transfectants were transduced with 300 and 3000 VP/cell of luciferase-expressing Ad35 vector for 1.5h. Forty-eight hours later, luciferase production was measured by luminescent assay. All data represent the mean ± S.D. of four experiments.

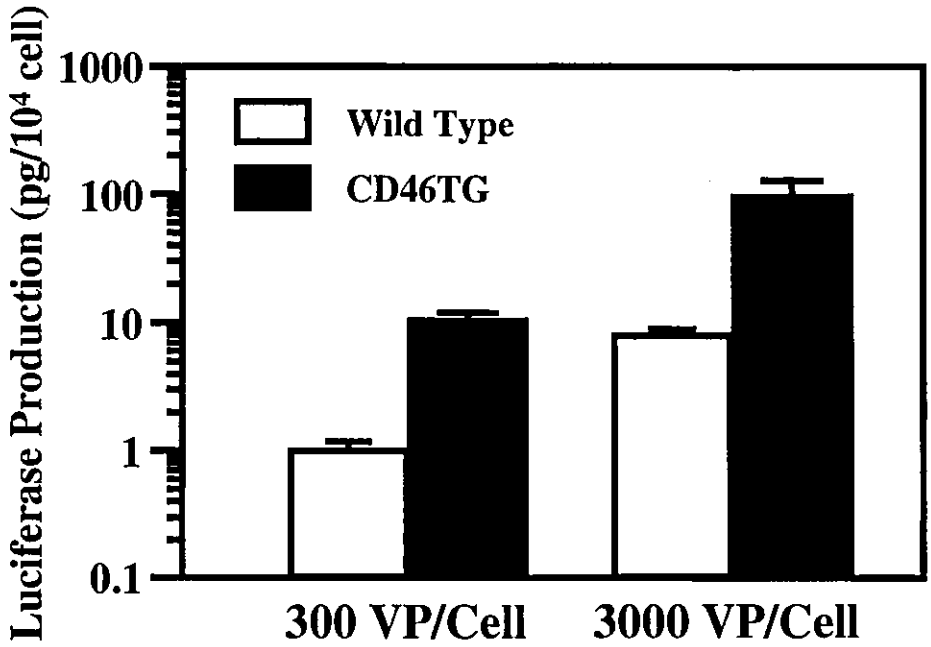

Fig.64 Ad35 vector-mediated transduction into mouse primary hepatocytes isolated from wild type mice and CD46-transgenic mice. Primary hepatocytes were recovered by collagenase perfusion and seed into Collagen-coated plates. The hepatocytes were transduced with 300 and 3000 VP/cell of luciferase-expressing Ad35 vector for 1.5h. Forty-eight hours later, luciferase production was measured by luminescent assay. All data represent the mean ± S.D. of four experiments.

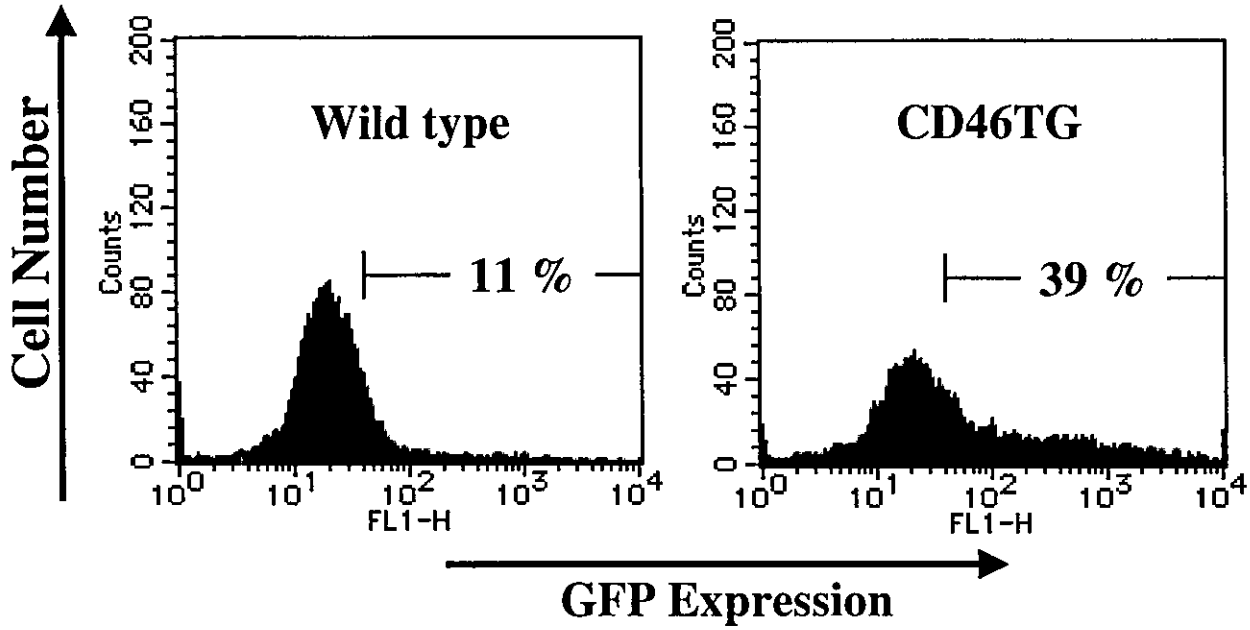

Fig.65 Ad35 vector-mediated transduction into mouse primary peritoneal macrophages isolated from wild type mice and CD46-transgenic mice. The macrophages were transduced with 3000 VP/cell of GFP-expressing Ad35 vector for 1.5h. Forty-eight hours later, GFP expression was measured by flow cytometer.

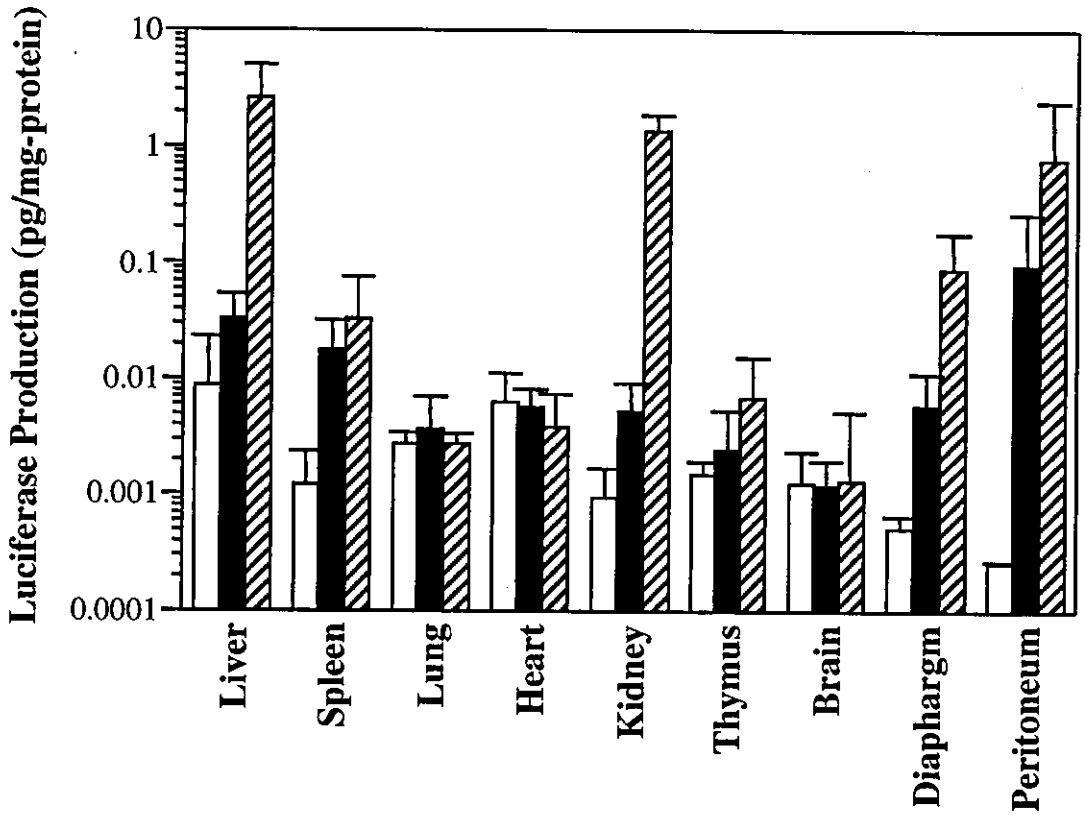

Fig.66 Ad35 vector-mediated transduction into CD46-transgenic mice after intraperitoneal administration. Luciferase-expressing Ad35 vectors were intraperitoneally administrated at a dose of 1.5×10^{10} VP/mice. Forty-eight hours after administration, the organs were harvested and luciferase productions were measured by luminescent assay. All data represent the mean ± S.D. of five experiments. Open bar; mock, Closed bar; wild type mice, hatched bar; CD46TG mice.

厚生科学研究費補助金(ヒトゲノム・再生医療等研究事業)

総括研究報告書

次世代アデノウイルスベクターの開発基盤研究

分担研究者　中川晋作　大阪大学大学院薬学研究科　助教授

本研究は、安全性が高く、機能面で優れたわが国独自の次世代遺伝子治療用ベクターの開発、および関連する遺伝子導入・発現技術に関する基盤研究を行うことを目的とする。その中で本年度は、サイトカインやケモカインを発現するファイバーミュータントアデノウイルス (Ad) ベクターを用いたがん遺伝子治療応用研究と、水溶性高分子 (PEG) によるバイオコンジュゲート化 Ad ベクターの開発を行い、以下の結果を得た。

1. サイトカインとケモカインを発現する改良型 Ad ベクターを用いたがん免疫遺伝子治療の最適化を図った。その結果、免疫系を活性化させるサイトカインとその細胞を腫瘍組織へ遊走させるケモカインを併用することで、活性化された抗腫瘍エフェクター細胞の腫瘍組織内への浸潤が増加し、強い抗腫瘍作用を得ることに成功した。
2. PEG ハイブリッド化 Ad ベクターを作製し、修飾率と体内動態および遺伝子発現の相関を検討し、その安全性・有用性評価を行った。その結果、PEG の修飾率に伴い血中滞留性が飛躍的に向上すること、PEG 修飾 Ad ベクターが抗体回避能を有すること、最適な PEG 修飾率を選択することで腫瘍組織に対する受動ターゲティングが可能であることを明らかにした。さらに、標的リガンドを PEG の末端に導入した PEG ハイブリッド化 Ad ベクターの作製方法を確立し、その有用性を明らかにした。

A. 研究目的

アデノウイルス(Ad)ベクターは、2004 年の時点で遺伝子治療臨床研究のプロトコール数あたりで約 26%を占めており、レトロウイルスベクターについで汎用されている。現存する遺伝子導入ベクターの中で、Ad ベクターの極だった特徴は、他のベクターに比べて極めて効率的かつ高い遺伝子発現を達成できる点にある。さらに非分裂期の細胞に対しても効率よく遺伝子導入できること、遠心により濃縮が可能であり、高タイターのウイルスが得られることなど、ベクターの基本的性質として多くの利点を有している。しかし一方で、遺伝子治療の重要なターゲットとなっている一部のがん細胞や血球系の細胞では、Ad の第一のレセプターである coxsackie-adenovirus receptor (CAR)の発現が無いあるいは乏しいため、Ad ベクターによる遺伝子導入に対して抵抗性を示し、遺伝子発現効率が極端に低い。そのため、これらの細胞を標的とする場合には、高濃度のベクターを適用しなければならず、そのためベクターによる非特異的な組織障害や過度の免疫反応を引き起こすことになる。また一方で Ad の感染域には組織特異性がないので、標的組織局所にベクターを投与してもその組織から漏れ出た Ad が他の組織や細胞に非特異的に移行してしまい、標的組織以外での過剰な遺伝子発現を招くことになる。また、Ad ベクターは血中投与後大部分が数分のうちに肝臓に集積するため、血液を介した腫瘍組織などへのターゲティングが困難であることや、Ad ベクターの抗原性による組織障害、抗原抗体反応による遺伝子導入効率の低下やアナフィラキシーショック等の問題がある。将来的に安全性と有効性を兼ね備えた Ad ベクターによる遺伝子治療を達成していくには、これらの問題点を同時に全て克服することが絶対的必須条件である。

我々はこれまでに Ad ベクターのファイバー領域に Arg-Gly-Asp (RGD) 配列を導入することに